# Determination of Rain Intensity from Doppler Spectra of Vertically Scanning Radar

Klaassen, Wim

*Published in:*
Journal of Atmospheric and Oceanic Technology

*DOI:*
10.1175/1520-0426(1989)006<0552:DORIFD>2.0.CO;2

# Determination of Rain Intensity from Doppler Spectra of Vertically Scanning Radar

WIM KLAASSEN

*Telecommunications Systems Group, Delft, The Netherlands*

(Manuscript received 23 March 1988, in final form 29 November 1988)

ABSTRACT

A new method is given to determine the rain intensity from data collected by a vertically scanning Doppler radar. The method is based on relating a theoretical velocity spectrum derived from a gamma drop size distribution to the measured Doppler spectra. A considerable reduction in calculation time is obtained by characterizing a Doppler spectrum by its total reflectivity and three velocities, and relating these parameters directly to the rain intensity, vertical air velocity and drop size distribution parameters.

The method is verified with observations of a high-resolution radar. A good agreement with the resulting rain intensity is found when large raindrops are present, but the accuracy of the method appears to reduce sharply in the absence of large raindrops. The Doppler spectrum shows a sudden decrease in reflectivity near the maximum fall velocity of raindrops when enough large drops are present. Without large drops, the Doppler spectrum appears hardly sensitive to the mean drop size, and any method that is based on an interpretation of the shape of the Doppler spectrum should be restricted to situations with large raindrops to produce accurate results.

## 1. Introduction

The relation between radar reflectivity and rain intensity depends on the raindrop size distribution. The size of the raindrops is related to the fall velocity, which can be derived from the Doppler velocity. A problem arises because the observed Doppler velocity is the result of the fallspeed of hydrometeors and of the vertical air velocity. To derive realistic results for the size distributions, the air motions have to be estimated or an assumption about the drop size distribution has to be made. In section 1a several existing methods using different assumptions will be analyzed, and in section 1b a modification of one of the methods is proposed.

### *a. Existing methods*

The vertical air motions can be estimated accurately close to the earth's surface (Pasqualucci 1984) or in light stratiform precipitation. In other situations an assumption about the drop size distribution has to be made.

The methods that are based on an assumption about the drop size distribution are divided according to the number of parameters to be solved. A method where the vertical air velocity and only one parameter of the drop size distribution are determined is called a two-parameter method. To derive two parameters of the drop size distribution (for instance $N_0$ and $\Lambda$ of an exponential distribution), a three-parameter method must be employed, and to derive the three parameters of a gamma distribution, four parameters must be solved.

Using a two-parameter method, the mean fall velocity can be calculated from the exponential drop size distribution as given by Marshall and Palmer (1948):

$$N(D) = N_0 \exp(-\Lambda D), \qquad (1)$$

where $N_0 = 8 \cdot 10^3\ \mathrm{mm^{-1}\ m^{-3}}$, $\Lambda = 4.1R^{-0.21}$, $D$ is the drop diameter in mm and $R$ is the rain intensity in mm hr$^{-1}$. By assuming a square root fall velocity-diameter relation according to

$$V(D) = 4.49D^{0.5}, \qquad (2)$$

where $V(D)$ is the fall velocity in m s$^{-1}$ of a raindrop with diameter $D$, Rogers (1964) found

$$V_z = 3.84Z^{1/14}, \qquad (3)$$

where $Z$ is the radar reflectivity in mm$^6$ m$^{-3}$ and $V_z$ is the (reflectivity weighted) mean fall velocity of the rain drops in m s$^{-1}$. With Doppler radar, the vertical air velocity $V_a$ can be calculated from

$$V_a = V_d - V_z, \qquad (4)$$

where $V_d$ is the (reflectivity weighted) mean Doppler velocity as measured by the radar in m s$^{-1}$.

According to Marshall and Palmer (1948) the rain intensity is related to the radar reflectivity through

$$Z = 200R^{1.6}. \qquad (5)$$

Equations (3) and (5) are denoted as "standard theory" in this study. One disadvantage of this method is that

*Corresponding author address:* Dr. Wim Klaassen, Telecommunications Systems Group 20-28, Dept. of Electrical Engineering, P.O. Box 5031, 2600 GA Delft, The Netherlands.

the Doppler spectrum is not used for supplementary information on the drop size distribution but only for the vertical air velocity. Natural variations in $N_0$ (Waldvogel 1974) may lead to important errors in the vertical air velocity.

Several authors (Sekhon and Srivastava 1971; Hauser and Amayenc 1980; Pasqualucci 1982 and Hodson 1986) proposed to recalculate the drop size distribution from the radar observations and a mean fall velocity similar to Eq. (3). The resulting drop size distribution was found to deviate from the a priori distribution; for instance, all studies end up with a lower value in the exponent of the $Z$–$R$ relation than assumed a priori. This may be caused by the small sensitivity of the reflectivity for small drops; consequently the measurement is likely to be affected by turbulence, crosstalk and noise.

The influence of noise can be limited by averaging, but averaging in time or space increases the influence of turbulence. The influence of turbulence can be kept small by averaging in the velocity domain. This can be done by reducing the velocity resolution or by characterizing the spectra by a restricted number of parameters.

As the two-parameter method is based on a fixed drop size distribution, it appears advantageous to increase the number of parameters that is determined from the Doppler spectrum. This can be done by calculating a second velocity, for instance the lowest velocity observed (Battan 1964) or the average of the lowest and highest velocity (Klaassen 1983). By using a second velocity, the shift of the Doppler spectrum due to air motions can be estimated and two parameters of the drop size distribution can be obtained independently. The lowest velocity method, however, is sensitive to the broadening of the Doppler spectrum (by turbulence for instance). Both methods calculate the second velocity from the low-reflectivity part of the spectrum, where the reflectivity is measured least accurately. Consequently these methods make very restricted use of the Doppler spectrum.

A three-parameter method that makes better use of the Doppler spectrum is given by Hauser and Amayenc (1981). Both parameters $N_0$ and $\Lambda$ of the drop size distribution and the vertical air velocity are least-square-fitted to the observed Doppler spectrum. One disadvantage of the fitting method is its long calculation time, which makes the method useless for real-time operation. To decrease the calculation time, a slightly different approach is proposed.

### *b. The three velocities (3V) method*

As compared to the fitting method, the 3V method uses the following modifications for speeding up:

1) Instead of using the complete (noisy) Doppler spectrum, the spectrum is represented by a few characteristic parameters.

2) The characteristic parameters are related to the rain intensity and vertical air velocity. These relations are simulated in advance so that during the observations the spectrum parameters can be related directly to the rain intensity and vertical air velocity.

To obtain the parameters of the exponential distribution the Doppler spectrum can be characterized by only three parameters. As noted by Sangren et al. (1984) the fitting procedure gives solutions for large and small drops. To discriminate between these solutions, a fourth parameter is included. The parameters that characterize the Doppler spectrum are chosen to be 1) The (total) reflectivity $Z$, 2) The mean Doppler velocity $V_d$, 3) The maximum Doppler velocity $V_x$, and 4) The median Doppler velocity $V_m$.

Because is uses three velocities, this method is referred to as the 3V method. Reflectivity and mean Doppler velocity are commonly defined. The maximum velocity is defined as the velocity at the upper part of the Doppler velocity spectrum, where the reflectivity has dropped 10 dB below the maximum value within this spectrum. The maximum velocity is chosen because the fall velocity of the raindrops exhibits a maximum for large drops where the fall velocity becomes almost independent of the drop size. Because of this, a sudden decrease (cutoff) of reflectivity with increasing Doppler velocity is often observed and the maximum velocity is used to mark the cutoff velocity. The median Doppler velocity is the velocity that separates the spectrum in two equal reflectivity parts. The median Doppler velocity is chosen to separate the solutions for small and large drops. The impact of these parameters is analyzed in more detail in section 2a.

By determining four parameters from the Doppler spectrum, it is possible to calculate the vertical air velocity and three parameters to characterize the drop size distribution. For the three-parameter drop size distribution, a gamma function is taken. The sensitivity of the method for deviations from the assumed drop size distribution is analyzed by truncating the distribution at a varying maximum drop size.

## 2. Theory

### *a. Representation of the Doppler velocity spectrum*

A common three-parameter representation of the drop size distribution is the gamma function

$$N(D)_{\text{gamma}} = N_0 D^m \exp[-(3.67 + m)D/D_0], \quad (6)$$

where $N(D)$ is the concentration of drops of size $D$ in $\text{mm}^{-1} \cdot \text{m}^{-3}$, $D_0$ is the median drop size, $m$ is the drop size dispersion factor and the factor 3.67 arises from $D_0 = (3.67 + m)/\Lambda$ (Ulbrich 1983). The parameter $N_0$ is a proportionality factor: the concentration of drops of all sizes is proportional to $N_0$; consequently the mean, median and maximum Doppler velocity are independent of $N_0$. This effect eases the conversion of

Doppler spectrum parameters to drop size parameters considerably and is further discussed in section 2c.

The influence of $D_0$ and $m$ on the Doppler spectrum and the three velocities is simulated by varying $D_0$ and $m$ over the range of interest for the observations in several steps. Unless otherwise stated $D_0$ is varied from 0.5 mm to 3 mm with increments of a factor 1.2 and $m$ from $-2$ (many smaller and larger drops) through 0, 2 and 4 to 6 (a small drop-size range); the range $-2 < m < 6$ is characteristic for the studies that were collected by Ulbrich (1983).

The simulations are performed with a smoothly truncated gamma function

$$N(D) = N(D)_{\text{gamma}} \times N(D)_{\text{trunc}}, \qquad (7)$$

where $N(D)_{\text{trunc}} = 1$ for $D < D_{\max} - \delta D$, $N(D)_{\text{trunc}} = 0$ for $D > D_{\max} + \delta D$ and $N(D)_{\text{trunc}}$ is linearly decreasing between these boundaries.

A truncation is included to analyze its influence on the Doppler spectrum and especially on the maximum Doppler velocity. Inclusion of a truncation is in agreement with disdrometer observations: Seliga et al. (1986) found on average $D_{\max} = 1.8D_0$, although this result is likely to be affected by the small measurement volume of the instrument (Joss and Gori 1978; Plank et al. 1980). To compensate for the small measurement volume a slightly larger value $D_{\max} = 2.0D_0$ is used in this study. When using $D_{\max} = 2.0D_0$ for $m = -2$ it appeared that approximately 75% of the reflectivity was deleted. This is a consequence of the sixth-power dependence of reflectivity with drop size and the relatively high concentration of large drops for distributions with $m < 0$. To prevent the deletion of so much reflectivity, the truncation is taken to be a function of $m$. We could not find any measurements on the dependence of $D_{\max}$ on $m$, or of the value of $\delta D$ and, unless otherwise stated, have arbitrarily taken the following values:

$$D_{\max} = 2D_0 f_m,$$
$$f_m = 5.67/(3.67 + m) \quad \text{and}$$
$$\delta D = 0.5D_0. \qquad (8)$$

The function $f_m$ has a unity value for $m = 2$ as the observations of Seliga et al. (1986) indicate on average the value $m = 2$. The drop size is converted to the fall velocity using the measurements of Gunn and Kinzer (1949). The Doppler spectrum appears very sensitive to the fall velocity relation and even the accurate representation by Atlas et al. (1973) results in significant changes in the Doppler spectrum at high velocities (see their Fig. 6) and thus in the computed maximum Doppler velocity.

Although the fallspeed relation would suggest an unique relation between drop size and Doppler velocity, one drop size may give reflectivity in a range of Doppler velocities. This phenomenon is called spectral broadening or (reflectivity) crosstalk. Spectral broadening is often ascribed to turbulence. In our situation where there is a very small observation volume and time, the influence of turbulence is very restricted. Broadening also arises from the digital Fourier transform of the radar signal and some from instabilities in the phase of the microwave radiation. These effects can be seen at the Doppler spectrum that arises from fixed targets (that have a constant zero velocity). From some spectra of fixed targets the spectral broadening is estimated for our radar system and included in the simulations. The value of the crosstalk of our radar system is given in section 3.

Figures 1–3 show the influence of the median drop-size $D_0$ and the drop size dispersion factor $m$ on the Doppler spectra. The values of the distribution parameters to be discussed below are given in the subscript of the figures; the value of $N_0$ results from the rain intensity that is taken equal for all curves. The figures are calculated assuming no vertical wind.

The values of $D_0$ in Fig. 1 are characteristic for rain intensities of 1, 10 and 100 mm/hr. The two curves of larger $D_0$ show almost the same maximum Doppler velocity, indicating the significance of $V_x$ to characterize the Doppler spectrum in situations of large raindrops. Note that the simulations are performed for $V_a = 0$, so a constant $V_x$ would imply that $V_a$ can be determined from a measurement of $V_x$ only; from $V_a$ the rain intensity and drop size distribution may be determined. The curves of larger $D_0$ are skewed towards high velocities whereas the curve of small $D_0$ is almost un-

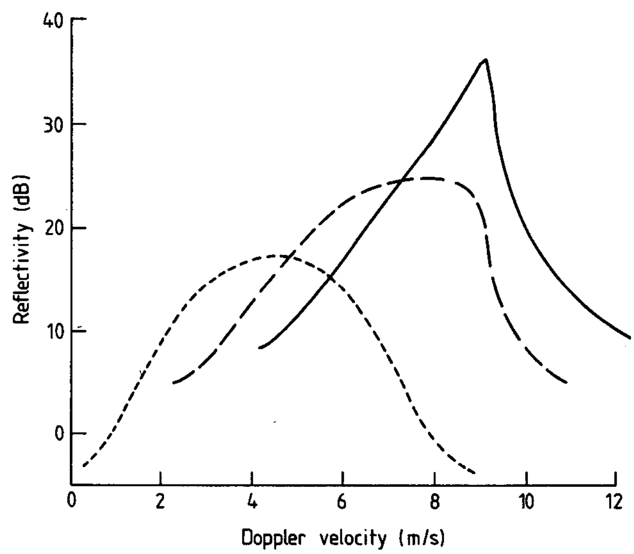


FIG. 1. Simulated Doppler spectrum of the truncated gamma distribution at $R = 10$ mm h$^{-1}$ with $m = 2$ for three values of the median drop size. The parameters $N_0$ (mm$^{-1}\cdot$m$^{-3}$), $D_0$ (mm), $Z$ (dBZ), $V_z$ (m s$^{-1}$), $V_x$ (m s$^{-1}$), and $V_m$ (m s$^{-1}$) for the dotted curve 3450836, 0.73, 29.2, 3.82, 5.83 and 3.88; for the dashed curve 14026, 1.64, 37.2, 6.74, 8.60 and 6.90; and for the solid curve 75, 3.70, 46.7, 8.76, 9.47, and 8.92.

skewed; the skewness will mark the significance of the median Doppler velocity $V_m$ for the data interpretation.

Figure 2 shows that the influence of the drop size dispersion factor on the Doppler spectrum is very similar to the influence of the mean drop size. The similarity is caused by the sensitivity of the Doppler spectrum for large raindrops. To show the difference between variations in $D_0$ and $m$, both parameters are varied in such a way that the total reflectivity is constant (Fig. 3). Then it appears that the dispersion factor influences the width of the spectrum; the influence on the skewness is much smaller.

In the presence of vertical air velocities the complete Doppler spectrum is shifted. As a result, the absolute value of one velocity is needed for the determination of the vertical air velocity and only the differences with the other velocities are necessary to determine the drop size distribution. To facilitate comparison with other studies, the mean Doppler velocity is used to calculate the vertical wind, using Eq. (4). The velocity differences are denoted by

$$V_x - V_d = W, \quad \text{the (upper) width and}$$

$$V_d - V_m = S, \quad \text{the (median) skew.} \qquad (9)$$

$W$ is called the upper width, as it measures the extension of the spectrum to high velocities. For a Gaussian distribution, $W$ is slightly larger than the $2\sigma$ width. Note that using the maximum velocity makes this method a kind of "upper-boundary" method. Just as the lower boundary and fitting methods, the 3V method

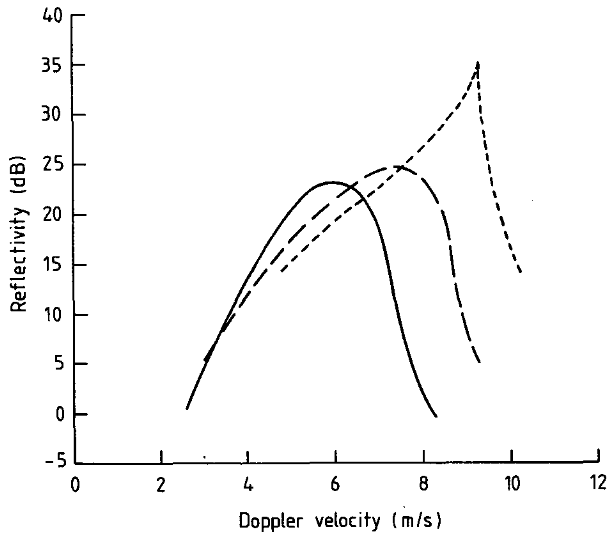


FIG. 2. Simulated Doppler spectrum of the truncated gamma distribution at $R$ = 10 mm h$^{-1}$ and $D_0$ = 1.64 mm for three values of the drop size dispersion factor. The parameters $N_0$ (mm$^{-1}\cdot$m$^{-3}$), $D_0$ (mm), $m$, $Z$ (dBZ), $V_z$ (m s$^{-1}$), $V_x$ (m s$^{-1}$), and $V_m$ (m s$^{-1}$) for the dotted curve are 995, 1.64, −2, 42.6, 8.39, 9.47 and 8.72; for the dashed curve 14026, 1.64, 2, 37.2, 6.74, 8.60 and 6.90; and for the solid curve 210818, 1.64, 6, 34.6, 5.65, 7.14 and 5.73.

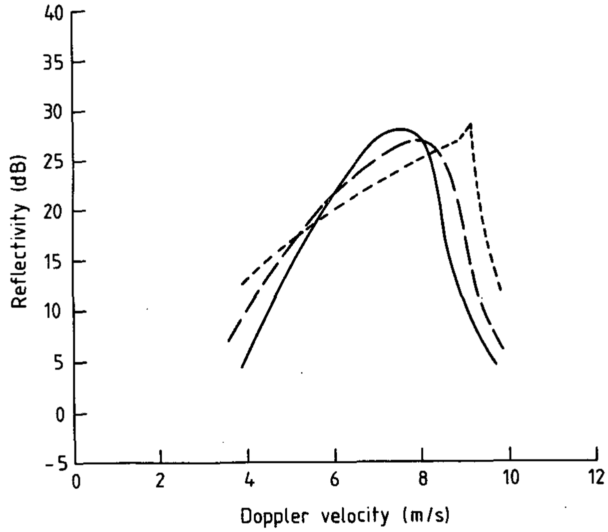


FIG. 3. Simulated Doppler spectrum of the truncated gamma distribution at $R$ = 10 mm h$^{-1}$ and $Z$ = 39 dBZ for three combinations of $D_0$ and $m$. The parameters $N_0$ (mm$^{-1}\cdot$m$^{-3}$), $D_0$ (mm), $m$, $Z$ (dBZ), $V_z$ (m s$^{-1}$), $V_x$ (m s$^{-1}$), and $V_m$ (m s$^{-1}$) for the dotted curve are 2547, 1.14, −2, 39.0, 7.75, 9.18, and 8.07; for the dashed curve are 5053, 1.92, 2, 39.0, 7.27, 8.98, and 7.44; for the solid curve are 3034, 2.45, 6, 39.0, 7.10, 8.44 and 7.20.

is sensitive to spectral broadening. In principle, the 3V method is sensitive to the noise level, just like the lower-boundary method. In practice however, with the maximum velocity set at the −10 dB level and a dynamic range in the Doppler spectra of more than 20 dB, the noise level is insignificant.

The median skew $S$ is related to the commonly defined skewness. The common skewness is proportional to the third power of the difference between the mean Doppler velocity and the velocity of the concerning reflectivity and thus most sensitive to the reflectivity far away from the peak, where the measurements are least accurate. The advantage of the median skew is its even sensitivity for the reflectivity of all velocities.

### *b. Relation between the Doppler spectral parameters and the drop size distribution parameters*

The relation between the spectral and drop size parameters is shown in Fig. 4 and reveals several essential features of the 3V method. In Fig. 4 the lower drop-size range is extended to $D_0$ = 0.2 mm. The figure is constructed with curves of constant median drop size and broken curves of constant drop-size dispersion of the truncated gamma distribution. The figure is independent of the value of $N_0$.

In Fig. 4 the upper width varies between 0.5 and 3 m s$^{-1}$ and the median skew between −0.05 and +0.35 m s$^{-1}$, so the variations in $W$ are an order of magnitude larger than the variations in $S$. This means that the variations in the drop size distribution are most clearly expressed in $W$. When decreasing $D_0$ (with $m$ constant)

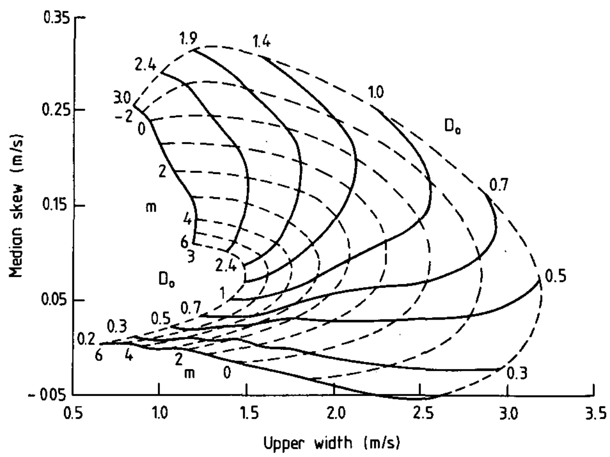


FIG. 4. Simulated upper width and median skew for the truncated gamma distribution for different values of $D_0$ and $m$.

from the largest to the smallest drops, $W$ is first found to increase. This is because the largest drops have about the same maximum velocity while the mean Doppler velocity is more sensitive to variations in $D_0$ (decreasing with decreasing values of $D_0$). This continues as long as there are enough large drops to give a −10 dB reflectivity near the maximum fall velocity. For distributions with smaller drops $W$ decreases again. This feature may explain why the fitting method using the correct fall velocity can give two solutions, one for large and one for small drops (Sangren et al. 1984). To distinguish between both solutions one may use the (small) deviation in $S$.

In three situations all reflectivity is found at only one Doppler velocity: for $D_0 \downarrow 0$ the size and velocity of all drop diminishes, for $m \uparrow \infty$ all drops have the size $D_0$ and for $D_0 \uparrow \infty$ all drops have the maximum fall velocity. In these situations a finite width is found in Fig. 4 because of the restricted velocity resolution and spectral broadening. In the limit $m \uparrow \infty$ the Doppler spectrum is independent of the value of $D_0$ and does not contain information on the size of the drops. For decreasing $m$ the range of $W$ and $S$ increases and the Doppler spectrum contains more information on the drop size distribution.

### *c. Comparison of the rain intensity as derived from the Doppler spectrum and from the differential reflectivity*

The method for determination of the rain intensity from the Doppler spectrum is elucidated by a comparison with the differential reflectivity ($Z_{dr}$) method. A brief explanation of the $Z_{dr}$ method is given first:

The basis of the $Z_{dr}$ method is the increasing flatness of falling water drops with increasing size. As a result the reflectivity of waves of horizontal and vertical polarization deviates (Seliga and Bringi 1976). $Z_{dr}$ is the ratio between the reflectivity at horizontal and vertical polarization and $Z_{dr}$ is a measure for the mean drop size. To analyze the potentials of the $Z_{dr}$ method and to compare it with the 3V method, a slightly different formulation of the basic equations will be given here. We start with the equations for reflectivity and rain intensity for the gamma distribution (Table 1, Ulbrich 1983):

$$Z = \frac{\Gamma(6 + m + 1)}{(3.67 + m)^{6+m+1}} N_0 D_0^{6+m+1} \tag{10}$$

$$R = \frac{\Gamma(3.67 + m + 1)}{(3.67 + m)^{3.67+m+1}} N_0 D_0^{3.67+m+1}, \tag{11}$$

where $\Gamma$ is the gamma function.
Dividing (10) by (11) results in:

$$Z/R = \frac{\Gamma(6 + m + 1)}{\Gamma(3.67 + m + 1)} (3.67 + m)^{(3.67-6)} D_0^{(6-3.67)}$$

or

$$Z/R = f(m) D_0^{2.33}. \tag{12}$$

Note that according to (12) $Z/R$ is independent of $N_0$ as $Z$ and $R$ are both proportional to $N_0$. So the value of $N_0$ is not important to calculate the rain intensity from the reflectivity when the drop size parameters are known. In the $Z_{dr}$ method $D_0$ is calculated from $Z_{dr}$ (see Fig. 2, Seliga and Bringi 1976 for instance) and thus $Z/R$ is calculated from $Z_{dr}$ by assuming a fixed value of $m$. Equation (12) shows that errors result when an incorrect value of $m$ is used (see also Fig. 8c, Ulbrich 1986).

Equations (11) and (12) are based on an approximate relation for the fall velocity of raindrops. Our simulation using the Gunn and Kinzer fall velocity measurements and the raindrop axial ratio measurements of Pruppacher and Pitter (1971) result in Fig. 5. The restricted number of points in Fig. 5 results

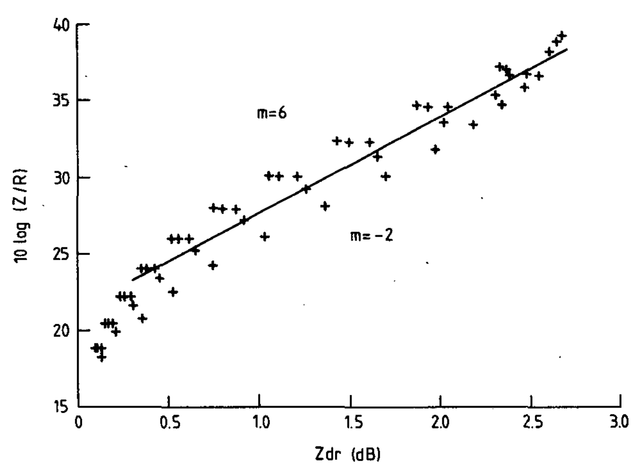


FIG. 5. The ratio between reflectivity and rain intensity vs. the differential reflectivity as simulated with the truncated gamma distribution. The scatter is mainly caused by variations in the drop-size dispersion factor. The fitted line represents $Z = 148 R Z_{dr}^{6.3}$.

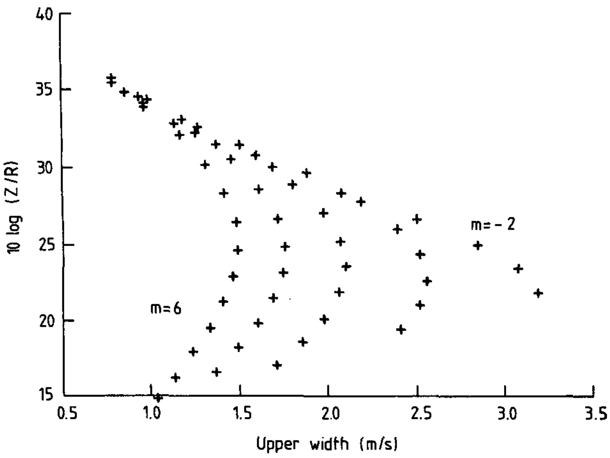


FIG. 6. The ratio between reflectivity and rain intensity vs. the upper width as simulated with the truncated gamma distribution.

from the selected combinations of $D_0$ and $m$ as given in section 2a. At a given $Z_{dr}$ the value of $Z/R$ increases with $m$, in agreement with Ulbrich (1986). For large $D_0$ this effect gets smaller as, apart from the truncation of (8), we used a sharp truncation at $D_{max} = 7$ mm. Assuming that the range $-2 \leqslant m \leqslant 6$ is realistic, the accuracy of the $Z_{dr}$ method can be estimated from the scatter of the simulated points around a best-fit line. For Fig. 5 this results in a rms scatter of 1.3 dB or 35%. For small $Z_{dr}$, or small drops, the sensitivity of $Z/R$ on $Z_{dr}$ increases, implying that a higher measurement accuracy is needed.

Calculation of the rain intensity with the 3V method is done in a similar way, but now we have two parameters $S$ and $W$ to account for the influences of $D_0$ as well as $m$ (see Fig. 4):

$$Z/R = f(m)D_0^{2.33} = f_1(W)f_2(S). \tag{13}$$

Note that, in accordance with the $Z_{dr}$ method, the 3V method does not use $Z$ to estimate $D_0$, though a statistical relation between $Z$ and $D_0$ is certain. The advantage of a method that uses more parameters is that an independent measurement is used instead of a statistical relation. A disadvantage of calculating $D_0$ and $m$ first is that, because of the complicated fall velocity relation, we could not find a simple analytical relation between the pairs ($S$, $W$) and ($D_0$, $m$). This problem is solved by skipping the second step of (13) and using a direct relation between $Z/R$ and ($S$, $W$). The functions $f_1(W)$ and $f_2(S)$ in (13) are simulated in a similar way as $f(m)$ in (12), using the same smoothly truncated gamma drop size distribution as used for Fig. 5. The result for $f_1(W)$ is shown in Fig. 6. The figure shows five curves for $m = -2$, 0, 2, 4 and 6. The curves coincide for large $Z/R$ or large drops and deviate for smaller drops. The deviation for small drops implies that the rain intensity cannot be determined from the reflectivity and upper width only. Figure 6 shows an upper level for $Z/R$ that decreases with increasing $W$. The upper level is found when large drops that have a large $Z/R$ are present; then an increase of $W$ means that, apart from the large drops, more smaller drops are present that result in a smaller $Z/R$. Deviations from this upper level are found when the distribution does not contain large drops and the maximum velocity of the Doppler spectrum does not coincide with the maximum fall velocity of raindrops. As a first guess, $f_1(W)$ is estimated from that part of Fig. 6 where the curves coincide.

The depence of $Z/R$, divided by $f_1(W)$, is shown versus the median skew in Fig. 7. The value of $f_1(W)$ is slightly changed from the first guess to reduce the scatter. The value of $f_1(W)$ is found from minimizing the scatter of $[\log(Z/R) - \log[f_1(W)]]$ versus $S$ for $S > 0.15$ m s$^{-1}$. The restriction $S > 0.15$ m s$^{-1}$ is included, as for smaller values of $S$ the Doppler spectrum is less useful to estimate the rain related parameters (see section 4a). For $S > 0.2$ m s$^{-1}$ the scatter in Fig. 7 is 0.5 dB or 12%, thus below the value as found with the $Z_{dr}$ method. This means that with a high $S$ or in the presence of large drops the 3V method can theoretically give results with a high level of accuracy.

For small $S$, Fig. 7 shows a strong dependence of $Z/R$ on the truncation. Different truncations were used to analyze the sensitivity of the 3V method on the drop size distribution (just as the sensitivity of the $Z_{dr}$ method was analyzed by varying the drop-size dispersion factor). The largest deviations occur for the distribution with a sharp truncation. Generally, we could not find significant deviations between Doppler spectra of a sharply truncated distribution and a concerning untruncated distribution with equal values of the 3V parameters. Both distributions show a sudden decrease of reflectivity around the maximum Doppler velocity

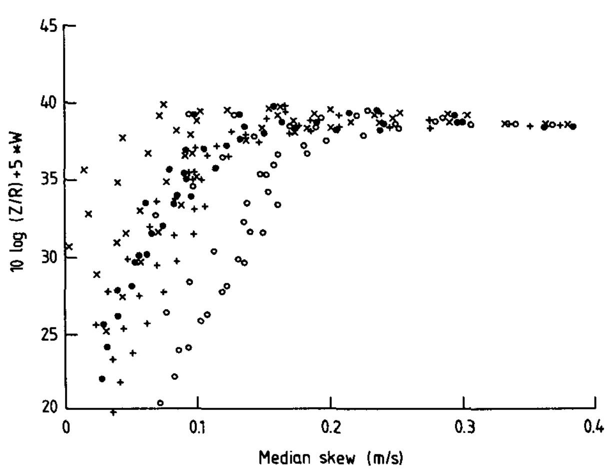


FIG. 7. The ration between reflectivity and rain intensity with the correction for the upper width of Fig. 6 vs. the median skew. The truncation parameters were set at: + $D_{max} = 1.5D_0$, $\delta D = 0.5D_0$; × $D_{max} = 2.0D_0$, $\delta D = 0.5D_0$; · $D_{max} = 3.0D_0$, $\delta D = .05D_0$; ○ $D_{max} = 2.0D_0$, $\delta D = 0.1D_0$.

that is interpreted as the maximum fall velocity using the 3V method. The large scatter for small $S$ (when few large drops are present) means that in these situations the results of the 3V method are extremely sensitive to the drop size distribution assumed. In the section on measurement results, it is reasoned that this result is not caused by a simplified characterization of the spectrum, but by the inexpressive shape of the Doppler spectrum in these situations.

In conclusion we find theoretically that both the $Z_{dr}$ and the 3V methods give satisfactionary results when large drops are present, with the 3V method less dependent on the drop size distribution assumed. In the absence of large drops, the results of both methods deteriorate, but more dramatically for the 3V method. The transition between accurate and inaccurate results of the 3V method is found around $S = 0.15$ m s$^{-1}$; this skew is characteristic for distributions with a reflectivity $Z \approx 35$ dB$Z$ or a rain intensity $R \approx 5$ mm/h$^{-1}$.

*d. Relations between the rain intensity, vertical air velocity and the 3V parameters*

The previous section gave an example of how the rain intensity can be derived from the 3V parameters. The vertical air velocity is found in a similar way by relating the mean fall velocity to $S$ and $W$ and then using Eq. (4). The simulations were done for the air density factor $\rho$ ranging from 0.5 to 1.1; $\rho$ being the ratio between the actual air density and the value at 1 bar and 20°C. The influence of air density has to be included, as the fall velocity depends on the air density and the density decreases with increasing height in the atmosphere. At decreasing air density the fall velocity increases. The dependence of the fall velocity on air density is calculated from Beard (1985). At decreasing air density the largest increase of fall velocity is found for the largest drops; consequently the reflectivity cutoff at large fall velocities is less sharp and so the upper width becomes less effective to characterize the Doppler spectrum. By varying $f_1(W)$ until a minimal scatter of $f_2(S)$ is found for $S > 0.15$ m s$^{-1}$ the following results for the rain intensity and vertical air velocity are obtained:

$$R = Z/[f_1(W)\cdot f_2(S)] \quad \text{with}$$

$$f_1(W) = 10^{[5(\rho-1)^3-(0.34+0.2\rho)W]}$$

$$f_2(S) = 10^{[3.96-12(S-0.295+0.06\rho)^2]} \tag{14}$$

$$V_a = V_z - V_d = f_3(W) + f_4(S) - V_d$$

$$f_3(W) = 9.81\rho^{-0.572} - (1.75 - 0.5\rho)W$$

$$f_4(S) = -(120 - 90\rho)\cdot(S - 0.275)^2. \tag{15}$$

Note that Eq. (15) does not show any dependence of $V_z$ on $Z$ or $N_0$, although a statistical relation between these quantities is certain; the reason for the absence of a mathematical dependence was discussed in section 2a. Equations (14) and (15) are derived for the velocity resolution and crosstalk level of the DARR radar and the same drop size distribution as used for Figs. 5 and 6. It is recommended to derive these equations again when a radar with other characteristics is available or when a strongly deviating drop size distribution is expected.

## 3. Measurements

The measurements are performed with the Delft Atmospheric Research Radar (DARR), described by Ligthart and Nieuwkerk (1980). This is a high resolution FM–CW radar. The main characteristics are:

| | |
|---|---|
| Center frequency | 3.315 GHz ($\lambda = 9$ cm) |
| Antenna beamwidth | 4.6 degrees (receiver)<br>1.8 degrees (transmitter) |
| Minimum range of full beam overlap | 0.5 km |
| Range resolution | 30 m |
| Doppler velocity resolution | 0.14 m s$^{-1}$ |
| Crosstalk to neighboring velocity bins | −6, −11, −15 dB and decreasing to −40 dB for distant bins |
| Observation time for a complete Doppler spectrum | 0.32 s |

To reduce noise, nine observations are averaged, resulting in a time resolution of 3 s. The radar observations are compared with a high resolution raingauge, situated 0.7 km east of the radar. For the comparison the average of the radar results between 650- and 800-m height interval are used. With westerly winds the rain in the radar-observed volume falls near the raingauge after approximately one minute.

The following events in 1987 are characterized in Table 1. The data for temperature and wind arise from measurements at 10 m height. The event of 6 August was situated at the edge of a shower; because of strong spatial variations, this event is not used for comparison with the raingauge.

## 4. Results

*a. The Doppler spectrum in rain*

Figures 8 and 9 show two examples of the observed Doppler velocity spectra together with some simulated curves. Figure 8 shows a skewed spectrum, characteristic for large drops and Fig. 9 a symmetric curve, associated with smaller raindrops. The reflectivity values are arbitrary so only the differences within the figures can be examined. Both figures show a dynamic range between 20 and 30 dB in the observations. We call the

TABLE 1. Observations.

| Day | Time (UTC) | Temperature (°C) | Wind dir. and speed (Dir., m s$^{-1}$) | Air pressure (mb) | Type of precipitation |
|---|---|---|---|---|---|
| 12 May | 1144–1158 | 10 | W, 4 | 994 | stratiform |
| 22 July | 0934–0945 | 17 | S, 2 | 1016 | stratiform |
| 6 August | 1221–2128 | 15 | W, 5 | 1015 | convective |

dynamic range the ratio between the reflectivity around the maximum and the reflectivity 4–5 m s$^{-1}$ separated from the maximum. With the maximum velocity defined at the −10 dB level, it seems that the dynamic range in the observations is sufficient for a reliable interpretation of the Doppler spectrum.

The simulated reflectivity, mean Doppler velocity and upper width are equal to the measured values; the simulated gamma distribution has also equal median skew. Figure 8 shows that with the parameters, given in the subscript of the figure, a good fit by eye to the observations has been made and that the quality of the fit is less sensitive to the median skew parameter. The rain intensity from the simulated exponential distribution deviates only 5% from the gamma distribution, in agreement with the small scatter of Fig. 7 for skewed spectra. The drop size dispersion factor $m$ took the values 0 and 4 in the simulated curves of Fig. 8, showing that $m$ cannot be measured accurately from a short measurement, in agreement with the simulations of Chandrasekar and Bringi (1987).

Figure 9 is compared with two exponential distributions that result in an equal upper width of the Doppler spectrum. The simulated distribution with small $D_0$ (0.63 mm) gives the best fit at small Doppler velocities and the distribution with higher $D_0$ (1.0 mm) at high velocities. Overall, both simulations are about equally good, but the simulation with small $D_0$ results in a 2.5 times larger rain intensity. Except for these exponential distributions, a realistic fit can also be obtained with numerous gamma distributions. This clearly demonstrates that the shape of almost symmetrical Doppler spectra can be fitted realistically by drop size distributions that deviate very strongly in the resulting rain intensity and vertical air velocity. So the poor results of the 3V method for unskewed spectra, as simulated in Fig. 7, is caused by the insensitive shape of those spectra for the dropsize distribution parameters and *not* by the characterization of the spectrum by only four parameters. As a result, interpretation on the shape should be restricted to spectra that are skewed towards large fall velocities. This conclusion has influenced the choice that is made for the parameters to characterize the Doppler spectrum:

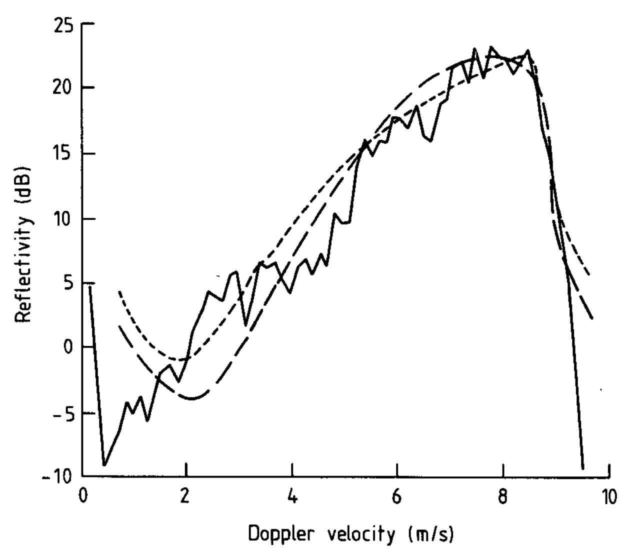


FIG. 8. Doppler velocity spectra. Solid curve: observed 0943 UTC 22 July 1987, at 700 m height and averaged over 3 and 30 m. Dashed curve: simulated gamma distribution: $D_0$ = 2.0 mm, $m$ = 4, $N_0$ = 7116 mm$^{-1}$ m$^{-3}$, $V_a$ = 0.8 m s$^{-1}$. Dotted curve: simulated exponential distribution; $D_0$ = 1.7 mm, $N_0$ = 1236 mm$^{-1}$ m$^{-3}$, $V_a$ = 0.7 m s$^{-1}$.

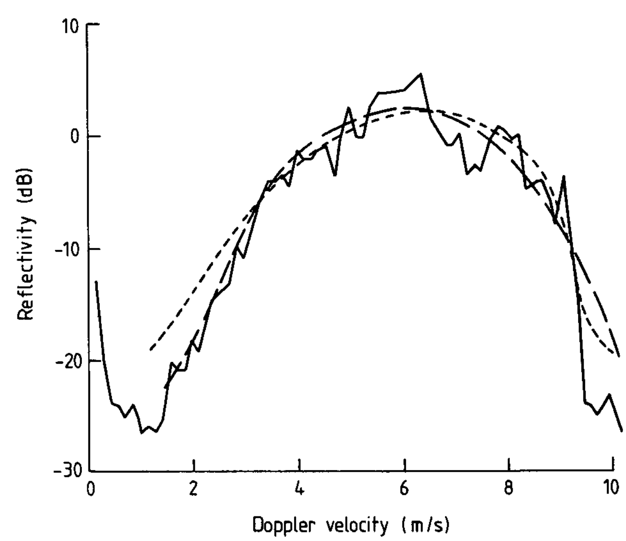


FIG. 9. Doppler velocity spectra. Solid curve: observed 1144 UTC 12 May 1987, at 880 m height and averaged over 3 s and 30 m. Dashed curve: simulated exponential distribution: $D_0$ = 0.63 mm, $N_0$ = 144081 mm$^{-1}$ m$^{-3}$, $V_a$ = 1.4 m s$^{-1}$. Dotted curve: simulated exponential distribution: $D_0$ = 1.0 mm, $N_0$ = 24342 mm$^{-1}$ m$^{-3}$, $V_a$ = 0.1 m s$^{-1}$.

1) Instead of using a commonly defined width, the upper width is selected as it appeared to result in a smaller scatter in $Z$–$R$ and $V_d$–$V_a$ relations when large drops are present. This result is a consequence of the insensitivity of the fall velocity on the drop size at large sizes (see section 2a).

2) The fourth parameter: the median skew is included to verify whether analysis of the spectrum shape is useful or not, although its influence on the resulting rain intensity is restricted in the situation of large drops (e.g., Fig. 7 hardly shows any dependence of $Z/R$ on $S$).

### b. The drop size distribution

Figure 10 shows the observed width and skew within the frame of the expected ranges from Fig. 4. The data points are averaged over 100 (10∗height and 10∗time) observations of 3 s and 30 m. Note that the width and skew are directly averaged, as these parameters are linear in the velocity spectra. This is an important advantage of the 3V method over nonlinear fitting methods.

The data of Fig. 10 are averaged to reduce the observational scatter. The scatter, caused by measurement uncertainties, is estimated by the scatter in series of 10 succeeding observations. In this way the observational scatter is slightly overestimated, as some meteorological scatter is also present in the observations of this time scale. The resulting sigma scatter is

$$\sigma W = 0.25 \text{ m s}^{-1}$$
$$\sigma S = 0.10 \text{ m s}^{-1}. \qquad (16)$$

When averaged over 100 observations, the scatter from measurement uncertainties is a factor 10 smaller and is insignificant. As a result the scatter in Fig. 10 can be attributed to variations in the drop size distribution. The data points fall within the frame of expected values. No points are found in the upper left of the figure, which is in agreement with the absence of high rain intensities during the observations. The event of 6 August is observed at the edge of a shower and is not believed to be typical for convective rain. The points in the lower left of the figure (indicating small drops) were observed during the final stage of the event of 12 May when the reflectivity dropped to values below 20 dBZ.

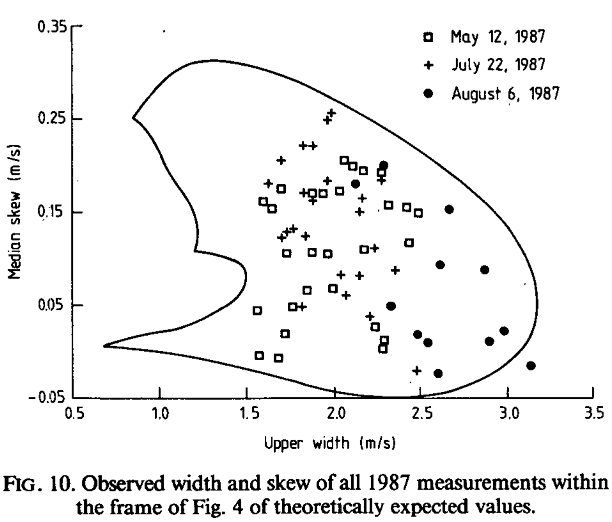


FIG. 10. Observed width and skew of all 1987 measurements within the frame of Fig. 4 of theoretically expected values.

Figure 10 indicates that the drop size dispersion factor is a constantly changing variable between the ranges −2 and 6. As a result the simulated scatter of 35% (Fig. 5) in the rain intensity, derived from the $Z_{dr}$ method, is expected to be realistic. To reduce that scatter, a project is started at the Delft University to measure the differential reflectivity and the width of the Doppler spectrum simultaneously from radar scans in an oblique angle. In this way an independent observation that is related to the drop size dispersion factor may improve the accuracy of the $Z_{dr}$ method.

### c. Rain intensity and vertical air velocity

The rain intensity of the stratiform events is compared with the raingauge results in Figs. 11–12. The figures show that it is possible to determine the rain intensity with a restricted scatter from the DARR observations by averaging over only 3 s. This is caused by the high data repetition time of the FM–CW radar. During the event of 12 May both the standard method and the 3V method gave accurate results. During the event of 22 July the 3V method shows unrealistic fluctuations during the first part of the event and the standard method resulted in a factor 2 overestimation of the rain intensity during the second part of the event. The largest fluctuations of the 3V method occur when the standard method underestimates the raingauge-derived rain intensity. An underestimation of the standard method might easily be caused by the presence of smaller drops than expected with that method. During the second part of this event the standard method overestimates the rain intensity, which can be explained by the presence of larger raindrops. Note that the variations in rain intensity are small, so variations in $N_0$ (Waldvogel 1974) are expected to surpass the influence of the rain intensity on the median drop size. Consequently we may expect relatively small drops during the first part of the event and large drops during the second part. The poor results of the 3V method during the first part of the event and the good results during the second part are thus in excellent agreement with the theoretically derived results of Fig. 7.

By averaging the data used for Figs. 11–12 over one minute, Fig. 13 shows that both the 3V and the standard method ($Z = 200R^{1.6}$) are equally accurate in determining the rain intensity and that both methods are unbiased within the limits of confidence. An averaging time of one minute was selected to account for

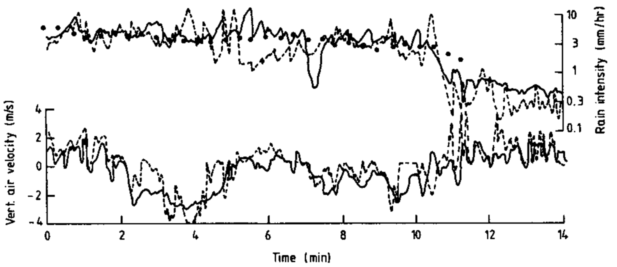


FIG. 11. Rain intensity and vertical air velocity at 700 m height from 1144 UTC 12 May 1987 onwards as derived from: standard theory (solid), 3V method (dash) and raingauge (dot).

the difference between the fastest falling drops ($V(D) \approx 9$ m s$^{-1}$) and the smallest drops with a high reflectivity ($D \approx 1$ mm, so $V(D) \approx 4$ m s$^{-1}$) to fall the vertical distance between both observation volumes. The rather high RMS error of 1.4 mm h$^{-1}$ is due to errors inherent to the method in situations of relatively small rain drops. The location of the raingauge (0.7 km east and 0.7 km below the radar observed volume) implies that an accurate verification is restricted to stratiform precipitation or westerly winds. At the location convective events are mostly accompanied with southern winds and the differences in rain intensity at both places of observation are generally too large for a useful verification. Consequently we could not verify the 3V method in the situation of a convective storm with large raindrops, where its results are expected to be most accurate.

## 5. Conclusion

The Doppler spectra are characterized by the total reflectivity and three velocities. These four parameters have the potential to determine three parameters of a gamma distribution of drop sizes and the vertical air velocity. A gamma distribution that fits the observed reflectivity and three velocities appears as a good fit to the complete Doppler spectrum. This means that the 3V parameters are an adequate alternative for the more complex nonlinear fitting method.

The parameters of the gamma distribution of drop sizes are determined graphically. An integration time of one minute was required to find the parameters with a realistic accuracy. The gamma distribution appears to fit the observed Doppler spectrum slightly better than an exponential distribution. In the presence of large drops the Doppler spectrum shows a sharp cutoff at high velocities and only one exponential distribution can be fitted realistically. Without large drops two strongly deviating exponential distributions and a broad range of gamma distributions can be fitted to the observations. As a consequence the radar-derived rain intensity and vertical air velocity is expected to be accurate in the presence of large drops only, or during events with moderate to high rain intensities.

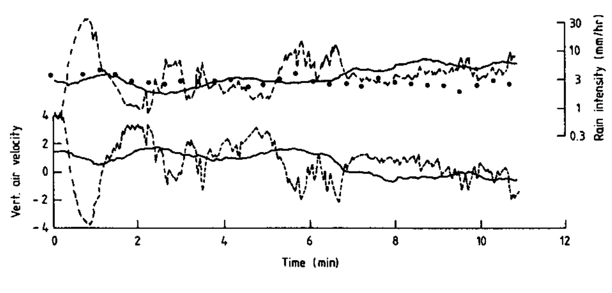


FIG. 12. As Fig. 11, but for 22 July 1987 from 0934 onwards.

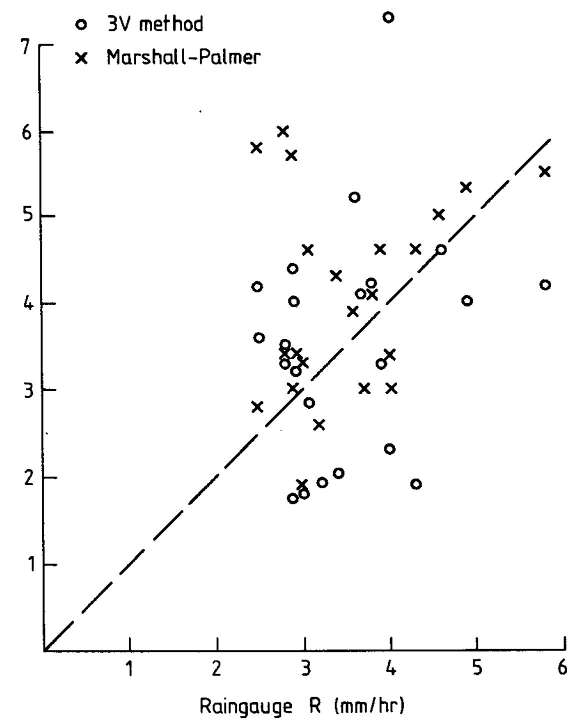


FIG. 13. Radar-derived rain intensity vs the raingauge value, both averaged over one minute for the 12 May and 22 July events.

The rain intensity of the 3V method and a standard method that uses an a priori relation between the reflectivity and rain intensity were compared with raingauge data. The rain intensity fell in the range between 2 and 6 mm/hr, around the lower limit for accurate interpretation of the Doppler spectra. On average the results of the 3V and the standard method are equally accurate. The accuracy of the 3V method improves when the observations indicate the presence of large drops and is better than the standard method in that situation. As a result the 3V method is recommended for use during high rain intensities.

The 3V method appears sensitive to the radar performance. For best results the radar should have a good stability (giving a large dynamic range in the Doppler spectra), a small measurement volume and time (decreasing the influence of turbulence) and a sufficient velocity resolution.

*Acknowledgments.* This study was supported by the Netherlands organization for Scientific Research (NWO). The progress of the research was discussed with L. P. Ligthart, Ph.D. and H. W. J. Russchenberg, M.Sc. The raingauge data were provided by Shape Technical Center and other meteorological data by the Royal Dutch Meteorological Office. The text was discussed with Prof. C. J. E. Schuurmans and J. C. van der Hage, Ph.D. and corrected by J. B. Zaat-Jones.

## REFERENCES

Atlas, D., R. C. Srivastava and R. S. Sekhon, 1973: Doppler radar characteristics of precipitation at vertical incidence. *Rev. Geophys. Space Phys.*, **11**, 1-35.

Battan, L. J., 1964: Some observations of vertical velocities and precipitation sizes in a thunderstorm. *J. Appl. Meteor.*, **3**, 415–420.

Beard, K. V., 1985: Simple altitude adjustments to raindrop velocities for Doppler radar analysis. *J. Atmos. Oceanic Technol.*, **2**, 468–471.

Chandrasekar, V., and V. N. Bringi, 1987: Simulation of radar reflectivity and surface measurements of rainfall. *J. Atmos. Oceanic Technol.*, **4**, 464–478.

Gunn, R., and G. D. Kinzer, 1949: The terminal velocity of fall for water drops in stagnant air. *J. Meteor.*, **6**, 243–248.

Hauser, D., and P. Amayenc, 1980: Drop-size distributions and vertical air motions in a thunderstorm as inferred from Doppler radar observations at vertical incidence. *J. Rech. Atmos.*, **3–4**, 439–455.

——, and ——, 1981: A new method for deducing hydrometeor-size distributions and vertical air motions from Doppler radar measurements at vertical incidence. *J. Appl. Meteor.*, **20**, 547–555.

Hodson, M. C., 1986: Raindrop size distributions. *J. Climate Appl. Meteor.*, **25**, 1070–74.

Joss, J., and E. G. Gori, 1978: Shapes of raindrop size distributions. *J. Appl. Meteor.*, **17**, 1054–61.

Klaassen, W., 1983: Accurate determination of vertical air velocities in rain by Doppler radar. *J. Climate Appl. Meteor.*, **22**, 1788–93.

Ligthart, L. P., and L. R. Nieuwkerk, 1980: FM-CW Delft Atmospheric Research Radar. *IEE Proc.*, **127F**(6), 421–426.

Marshall, J. S., and W. M. K. Palmer, 1948: The distributions of raindrops with size. *J. Meteor.*, **5**, 165–166.

Pasqualucci, F., 1982: The variation of drop-size distributions in convective storms: A comparison between theory and radar measurements. *Geophys. Res. Lett.*, **9**, 839–841.

——, 1984: Drop size distribution measurements in convective storms with a vertically pointing 35 GHz Doppler radar. *Radio Sci.*, **19**, 177–183.

Plank, V. G., R. O. Berthel and L. V. Delgado, 1980: The shape of raindrop spectra for different situations and averaging periods. *J. Rech. Atmos.*, **14**, 301–309.

Pruppacher, H. R., and R. L. Pitter, 1971: A semi-empirical determination of the shape of cloud and raindrops. *J. Atmos. Sci.*, **28**, 86–94.

Rogers, R. R., 1964: An extension of the $Z$–$R$ relationship for Doppler radar. *Proc. 11th Weather Radar Conf.*, Boulder, Amer. Meteor. Soc., 158–169.

Sangren, K. L., P. S. Ray and G. B. Walker, 1984: A comparison of techniques to estimate vertical air motions and raindrop size distributions. *J. Atmos. Oceanic Technol.*, **1**, 152–165.

Sekhon, R. S., and R. C. Srivastava, 1971: Doppler radar observations of drop size distributions in a thunderstorm. *J. Atmos. Sci.*, **28**, 983–994.

Seliga, T. A., and V. N. Bringi, 1976: Potential use of radar differential reflectivity measurements at orthogonal polarizations for measuring precipitation. *J. Appl. Meteor.*, **15**, 69–76.

——, K. Aydin and H. Direskeneli, 1986: Disdrometer measurements during an intense rainfall even in Central Illinois: Implications for differential reflectivity radar observations. *J. Climate Appl. Meteor.*, **25**, 835–846.

Ulbrich, C. W., 1983: Natural variations in the analytical form of the raindrop size distribution. *J. Climate Appl. Meteor.*, **22**, 1764–1775.

——, 1986: A review of the differential reflectivity technique of measuring rainfall. *IEEE Trans. Geosci. Remote Sens.*, **6**, 955–965.

Waldvogel, A., 1974: The $N_0$ jump of raindrop spectra. *J. Atmos. Sci.*, 1067–1078.